International Journal of Thin Films Science and Technology

http://dx.doi.org/10.12785/ijtfst/040211

Annealing Temperature Dependence on Structural, Electrical Optical and Photoluminescence Properties of Nanocrystalline CIO Thin Films

***P. Deepa, V. Sivaranjani* and *P. Philominathan**.**

PG and Research Department of Physics, AVVM Sri Pushpam College (an autonomous institution affiliated to Bharathidasan University, Trichy), Poondi, Thanjavur 613 503, India.

Received: 18Feb. 2015, Revised: 5Apr.2015, Accepted: 8Apr.2015.
Published online: 1 May 2015.

Abstract: In this work, we have reported the effect of annealing temperature on structural, optical, electrical, and photoluminescence properties of the nanocrystalline copper doped indium oxide thin films prepared by simplified spray pyrolysis technique using perfume atomizer. XRD reveals that the films are polycrystalline with cubic structure. Photoluminescence was also measured at room temperature and the spectrum confirms the deep-level as well as near band edge emission. From the optical measurements, optical constant of this films calculated by a recently introduced method of calculations, PUMA. The absorption coefficient, refractive index and extinction coefficient are obtained for prepared films. The negative sign of hall co-efficient confirmed n-type conductivity. Films with high mobility of 14.5 $cm^2/(Vs)$, carrier concentration of 1.9 $\times 10^{20}$ cm^{-3}, resistivity of $2.27\times10^{-4}\,\Omega$cm were obtained when annealed at 400 K..

Keywords: Thin films, XRD, Annealing temperature, Perfume atomizer method.

1 Introduction

The orgin of transparent conducting Indium oxide (In_2O_3) thin film which presents a high conductivity (free carriers upto 10^{17}to10^{19} cm^{-3}) without intentional doping is still under debate [1,2]. Moreover, undoped In_2O_3 thin films exhibit conductivities with 45 orders of magnitude higher than that of the bulk [3], because of the presence of surface donors devoid of bulk defects. When doped with typically 9 at.% tin oxide, indium-tin oxide(ITO) becomes one of the most popular transparent conducting electrodes that find application in thin film photovoltaic's, flat-panel display devices, due to the highest transparency for visible light(>85% at wavelengths from 340 to 780 nm) combined with the lowest electrical resistivity ($7.7\times10^{-5}\,\Omega$ cm) [4]. The recent trend towards higher quality transparent conducting electrodes, constraints to specific electronic and solar cell technologies demands that continuous optimization of In_2O_3 thin film properties and processing conditions [1,2].

Photovoltaic devices have attracted increasing attention as an effective and sustainable energy source. The energy conversion efficiency of photovoltaic devices depends closely on the band gap energy of the light-absorbing layer integrated into the photovoltaic devices [5]. Copper oxide (CuO) is a p-type semiconductor with an in-direct transition [6]. The band gap energies of CuO films, however, ranged from 1.3 to 1.9 eV depending on the preparation process and conditions [7-8]. CuO has been used as gas and humidity sensors [9-10], dye-sensitized solar cells [11], and as a catalyst. If the ideal band gap energy of around 1.4 eV could be achieved, CuO could be a potential candidate for an ideal light absorbing layer. The CuO films have been prepared by several techniques, such as radio-frequency magnetron sputtering [12], thermal oxidation [13], and electrodeposition [14-15]. In the present study, copper doped indium oxide films were prepared by simplified spray pyrolysis techniques. Here, a simple and elegant technique employing a perfume atomizer has been chosen to deposit copper doped indium oxide thin films and to the best of our knowledge the study of nanocrystalline CIO thin films using simplified spray pyrolysis [16] has not yet reported.

2 Materials and methods

Nanocrystalline copper doped indium oxide thin films synthesized by simplified spray pyrolysis technique using perfume atomizer. The indium III chloride ($Incl_3$) was used as the source for indium, whereas the copper doping

*Corresponding author e-mail: philominathan@gmail.com

was achieved using copper acetate (Cu). Microscopic glass plates (25× 25 ×1.2 mm^3) cleaned by acetone was used as substrate. Indium tricholoride was dissolved in 2 ml of concentrated HCL acid by heating it at 500^0 c for 10 min. The resultant transparent solution diluted with methanol forms the starting solution. For copper oxide, the required amount of Cu-Ac was dissolved in double distilled water. Then these two solutions were mixed together by vigorous stirring to get a transparent solution which is well suited for deposition processes, the substrate temperature (250 K). Deposited samples were annealed at different temperatures ranging from 300 to 400 K. All the CIO films were annealed for 1 hour. The X-ray diffracrometer (PANalytical PW 340/60 X' pert PRO) which operates at 40 KV and 30 m A with CUK radiation (λ =1.5405 Å) was used to record the X-ray diffraction (XRD) patterns. The transmission data were observed in the range of 300-1100 nm using ultraviolet visible near infrared double beam spectrophotometer (Perkin Elmer Lambda 35 model). The electrical properties were studied with the use of Hall Effect apparatus (ECOPIA HMS-3000) with van der pauw configuration and the spectro- flurometer (Jobin Yvon-FLUROLOG FL3- 11) with Xenon lamp (450 W) as the excitation source of wavelength 325 nm was used to record the photoluminescence spectra of the films at the room temperature.

3 Results and Discussion

3.1 Structural Properties

XRD patterns of copper doped indium oxide thin film annealed at different temperature along with that of an as-prepared sample were shown in Fig. 1. Well defined peaks at 22^0 corresponding to reflection (2 1 1) plane was observed in as-deposited sample. This indicates that all samples are polycrystalline and matched the characteristic peaks of the cubic In_2O_3 phases (JCPDS 00-06-0416). Annealing the samples at temperature up to 300 K show a preferred orientation along (2 2 2) direction corresponding to cubic phase of indium oxide. The strong diffraction peaks of the films changed from the (2 1 1) to plane to the (2 2 2) plane. If the respective ion, the change in the preferred orientation may not occurs. However, if the dopant occupies additional interstitial sites which are unoccupied, a change in the preferred growth takes place. In the present study it seems that Mo replaces indium at its regular lattice sites annealed at 300 K. The Mo incorporated at additional interstitial sites changes the preferred orientation of the films. The change in preferential orientation was also observed in Sn doped In_2O_3 films by Agashe and Mahamuni [17]. For the samples annealed at 350 K, XRD pattern shows three more extra peaks which are found to be in In_2O_3 phases. The $2\theta = 35^0$, 46^0 and 51^0 represents the plane (4 0 0), (4 3 1) and (4 4 0) respectively. But in the XRD patterns of cubic In_2O_3, phases of (4 0 0), (4 3 1) and (4 4 0) are very less intense compared to (2 2 2) plane. Many of the reports show that the intensity of preferred orientation of crystalline growth strongly depends on the deposition condition of the film. When the samples are annealed at 400 K, the same diffraction planes and phase are appeared. Further, three more peaks at $2\theta = 21^0$, 61^0 and 65^0 for (2 1 1), (6 2 2) and (5 4 3) planes which corresponds to indium Oxide phase are observed.

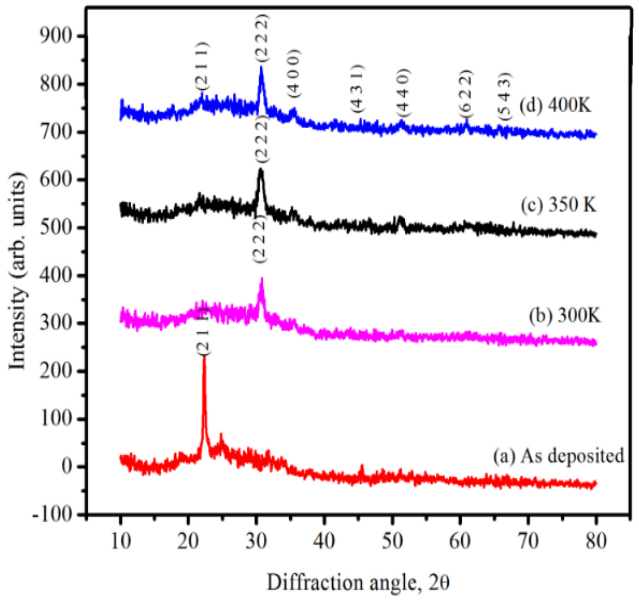

Figure 1: XRD patterns of as-deposited and annealed CIO thin films at various annealing temperatures.

All the films does not show any CuO peaks indicating that CuO is well dispersed in the In_2O_3 lattice. The ionic radius of In^{3+} in In_2O_3, is 8.1× 10^{-11} m, and that of Cu^{2+} is 7.3 ×10^{-11} m. So it is possible for Cu^{2+} to substitute In^{3+} in In_2O_3 [18]. The planes of CIO films fairly coincide well with JCPDS data [00-035-1150]. The intensity of diffraction peak has increased as the annealing temperature increased upto 400 K. The XRD patterns of as-deposited and annealed CIO films show the presence of diffraction planes which are not reported in earlier work. The increased peak intensity from as-deposited to annealed films may attribute to the continuous increase in film thickness. The crystalline grain size was estimated using the Debye-Scherrer equation. The average crystalline size was found to be 20 nm for the as deposited CIO films and it was increased to 66 nm after annealing at 400 K. The increase in D value after annealing might be due to decrease in grain boundaries, and hence the amount of defects in the films. The thermal energy produced by annealing led to the enhancement in the mobility of active species by filling the micro-voids or defects in the structure and also for the formation of more packed and large crystalline films Park et al [19]. The result imply that the grain size of nanocrystalline thin films size increases with increasing annealed temperature, the same tendency was observed by Changhyun et al [20], Joseph et al [21].

3.2 Electrical properties

The electrical resistivity (ρ), carrier concentration (n) and hall mobility (μ) of both type of CIO thin films (as-deposited and annealed) deposited at different annealed temperature of In_2O_3 were measured. The Hall measurements were performed at room temperature in van der pauw configuration. The negative sign of Hall co-efficient confirmed n-type conductivity. Fig. 2(a,b,c) summarizes electrical resistivity results of as-deposited and annealed CIO thin films. The ρ of the as-deposited films is significantly decreased from 7.61 to 6.41×10^{-3} Ω cm when it is annealing at 300 K. ρ is then gradually decreased with an increase in annealing temperature 350 K to reach 3.8×10^{-3} Ω cm. When the annealed temperature is increased further to 400 K, this moderately decreased to 2.27×10^{-3} Ω cm. On the other hand a low n 0.85×10^{20} cm^{-3} obtained for the as-deposited films is significantly increased to 0.95×10^{20} cm^{-3} for annealed films at 300 K. However, further increased in the annealing temperature 350 K leads to a gradual increase in the carrier concentration to reach the maximum of 1.2×10^{20} cm^{-3}. The increase in n is due to the increasing annealing temperature and desorption of oxygen produced by high temperature vaccum annealing. A high n of 1.9×10^{20} cm^{-3} (annealed at 400 K) further enhances and creates more free electrons resulted in to an increase in carrier concentration. Obtained in the present study is nearly one order of magnitude lower than that of typical polycrystalline indium tin oxide (ITO) thin films [22]. A minimum μ of 4.8 (cm^2/Vs) observed for the as deposited films is increased significantly to 10.2 (cm^2/Vs) annealed at 300 K and then gradually increased to 13.7 (cm^2/Vs) when annealed at temperature 350 K. The increase in mobility (μ) with the increasing annealing temperature to reach the maximum value of 14.5 (cm^2/Vs) obtained in annealed at 400 K. It can be noted from figures that the resistivity of as-deposited CIO thin film decreases with the increasing annealed temperature upto 400 K can be attributed to the increase in the carrier concentration and the mobility of the charge carriers. In CIO thin films, the In_2O_3 may diffuse into CuO matrix. Due to difference in their grain sizes, diffusion of In_2O_3 in CuO matrix causes an increase in free interstitial lattice spaces. The mobility of valance electrons is increased in the free spaces and increase in mobility causes the decreases in resistivity. In addition to this, being less electronegative than copper (Cu), indium (In) atoms behave as donors and enhance the carrier concentration. Further, the oxygen vacancies also play a very important role in the electronic properties of CIO thin films. Oxygen vacancies like defects are the primary source of charge carriers. The usual description of Oxygen-vacancy doping in crystalline CIO thin film using Kreoger-Vink notation is given as

$$o_o^x = \frac{1}{2}o_2(g) + V_0^{\cdot\cdot} + 2e^- \quad (1)$$

Which indicates that the oxygen on the oxygen sub-lattice (o_o^x) is lost as oxygen gas (o_2) creates a doubly charge oxygen Vacancy ($V_0^{\cdot\cdot}$) with two free electrons [23-24], hence increases the concentration of charge carriers. As the number of charge carriers increases, resistivity decreases. It can be observed from Fig. 2(a) that the film shows comparatively low resistivity and high conductivity when annealed at 400 K. The increase in the electrical conductivity is due to the presence of large number of free carriers introduced during annealing period [25].

Consequently, higher annealing temperature is led to the formation of lower resistance or higher conductivity films. This is basically due to the mobility increase in (or) carrier density at high annealing temperature and hence could be attributed to the improved crystalline nature of films. The electrical property of the films is found to be related to the crystalline nature, which in turn strongly depends on the annealing temperature.

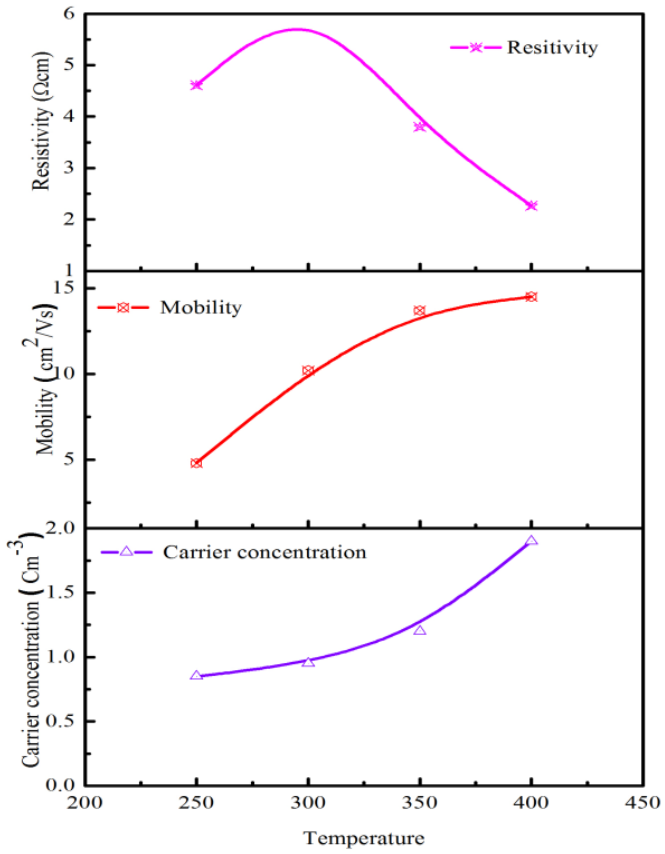

Figure 2: (a) Resistivity (b) hall mobility (c) carrier concentration of the as-deposited and annealed CIO films.

3.3 Photoluminescence properties

The analysis of photoluminescence (PL) spectroscopy at room temperature reveals various peaks as shown in Fig. 3(a,b). We use the photoluminescence spectroscopy to

determine the band gap of semiconductor and since the most common radioactive transition in the semiconductor occurs between starts at the bottom of the conduction band and the top of the valance band [26]. The emission properties of as-deposited and annealed films were studied by using PL spectra excited wavelength at 350 nm. The as-deposited film of sample 520 nm shows very broad PL spectral features compared to the annealed films. The spectrum of the as deposited film shows peaks centered at 528 nm, with a shoulder at 398 nm. In general, emission spectra can be divided into two broad categories: the near-band edge (NBE) emission and deep level (PL) emission [27]. High crystal quality and the quantum confinement effect related to the nanostructures are the two factors favoring the increase in the intensity of UV emission at room temperature. High crystal quality of CIO films may be attributed to the annealing process. This can decrease impurity and structural defects such as oxygen vacancies. This lead to a high NBE-emission to DL emission ratio, which results in a detectable UV emission at room temperature [28-29].

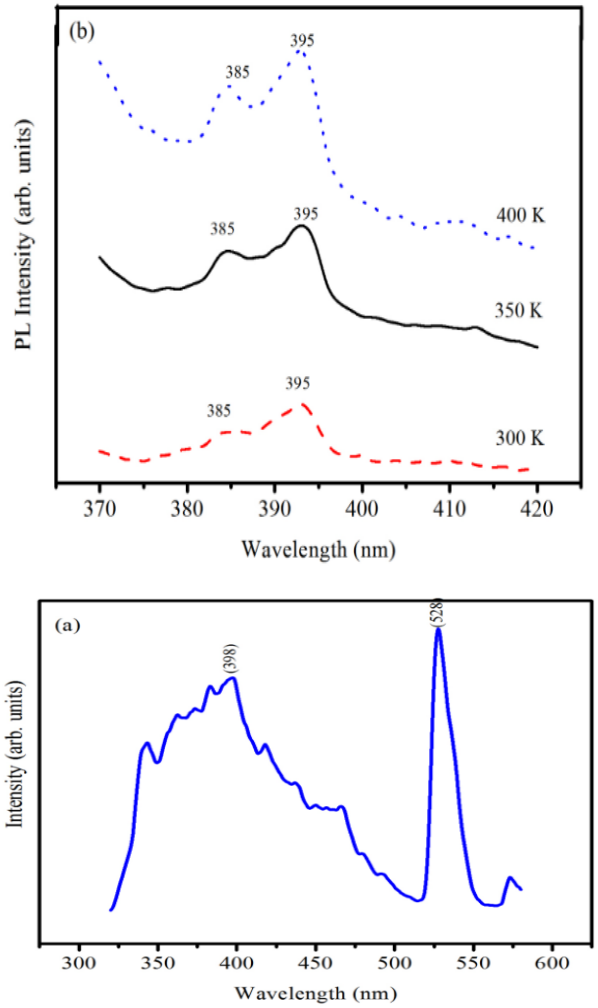

Figure 3: As-deposited (b) annealed photoluminescence spectra of CIO thin films.

The copper doped indium films particularly the as deposited film contains large number of defect and due to oxygen vacancies can induce the formation of energy levels in the energy band. The blue emission from pure In_2O_3 film resulting from the radioactive recombination of electrons occupying oxygen vacancies with a photo-excited hole, which is analogous to the PL mechanism of ZnO and SnO_2 semiconductors [30]. The samples at 300 K shows near band edged emission peak in the visible region centered at 393 nm and 384 nm. The position of the PL peak remained unchanged with the increase in annealing temperature but the emission intensity of the peak changes. The intensity of blue NBE emission depends strongly on the annealing temperature. When the annealing temperature are at 350 and 400 K, the thin films exhibits more intense blue emission than as-deposited film, and the intensity of blue NBE emission increases with further increase the annealing temperature (400 K). The blue NBE emission spectra from exciting related recombination [31-32]. Upto now, there is no clear explanation for the PL mechanism in CIO thin films. One of the generally accepted mechanism is the quantum confinement effect- since the diameters of the nanofilms is larger than that of the critical Bohr radius of In_2O_3 (2.38 nm [33]), the quantum confinement effect is ignored. The other generally accepted mechanism is the defect related emission. For the rapid evaporation, deposition and oxidation process companying the 200 sccm carries gas argon, there may be no enough supply of oxygen and the defects related to oxygen vacancies usually act as deep defect donors in semiconductors, deep energy levels can be formed in the band- gap in the In_2O_3nanowires [34]. The PL light emitting property in the UV region at room temperature suggests possible the applications of these films in nanoscale upto electronic devices in the future.

3.4 Optical properties

Determination of the optical constants has been absorption coefficient(α), refractive index (n) and extinction coefficient(k) perhaps one of the most challenging tasks, when studying the optical properties of materials since this involves complex equations and a great deal of computing. A number of methods and different approaches exist to determine the optical constants. The easiest of them are those, which depend on single transmittance measurement. Absorption coefficient, refractive index and extinction co-efficient of the CIO thin films studied here were determined from the transmittance data only using PUMA approach and software [35]. Point-wise unconstrained minimization approach (PUMA for the estimation of the optical constant n, k and α of thin films) software is a procedure described by Birgin et al [35]. This method implements the complex optical equations, shown below, derived and formulated by Heavens [36] and Swanepoel [37]. In PUMA, the experimental transmittance obtained for the film is compared with a theoretical value. The difference

between the two values is minimized until a best solution is reached for the refractive index, absorption co-efficient and extinction co-efficient Poelman and Smet [38] have reviewed and tested this method independely and shown it that produces excellent estimates of optical parameters of thin films. The absorption is an important parameter for characterizing the penetration depth of the light waves into the thin film layers. The optical absorption of CIO as-deposited and annealed films was studied in the range 200-1100 nm. Fig. 4 shows the variation of absorption with wavelength. As can be seen in Fig. 4 especially a, b and c films have low absorption co-efficient at high wavelengths compared to the other films.

We think that this may be a result of their high transmission values. The absorption decreases with increases in wavelength range 300-1100 nm for a, b and c samples. But d sample have high absorption co-efficient value at 300 nm. The absorption of the film is found to be increase with increasing annealed temperature upto 400 K. This is possibly due to the increase in the crystalline nature and decrease in the number of defects in the localized state [39]. Also, for the samples are annealed at 400 K, the absorption is slightly changed depending on the change in the crystalline nature. The refractive index can be considered as a fundamental property of a material, because it is closely related to the electronic polarizability of ions and the local field inside the material. The refractive index of CIO as deposited and annealed films was studied in the wavelength rage 300-1100 nm as shown in Fig. 5. The refractive index of the as deposited films is significantly increased from 3.1 to 3.8 when annealed at 300 K.

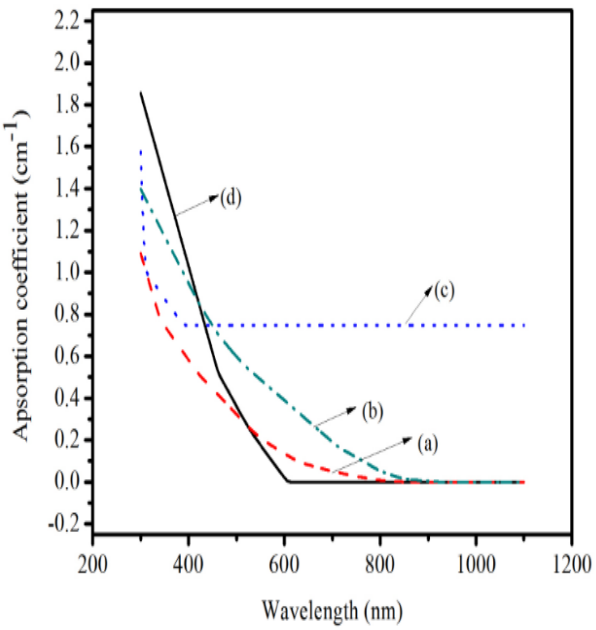

Figure 4: Annealing effect on absorption co-efficient of copper doped indium oxide thin films.

Refractive index is then gradually increased with an increase in annealed temperature 350 K to reach 5.9. When the annealing temperature is increased further to 400 K, the

refractive index is slightly increased beyond 6.2. Hence, refractive index increases with increase in annealing temperature. The low values of the refractive index of the films indicate that these films had relatively low packing density. Lowering of the packing density is caused by the incorporation of oxygen during film growth [40], which may create voids that absorb moisture [41]. Moreover, collision of the evaporated species with O_2 molecules reduce their kinetic energy before reaching the substrate, and this will result in lower packing density [41]. The increase of refractive index with annealing temperature may be attributed to an increase in the density of films deposited on heated substrates. Substrate heating provides thermal energy that increases the mobility of the atom of the films thereby increasing the packing density of the films [42]. In particular, the higher values of the refractive index binary films suggest the application of the films in opto-electronic industry.(The reason for maximum value of refractive index particularly film annealed at 400 K was due to the samples has high optical transmittance which is shown in transmittance spectrum)

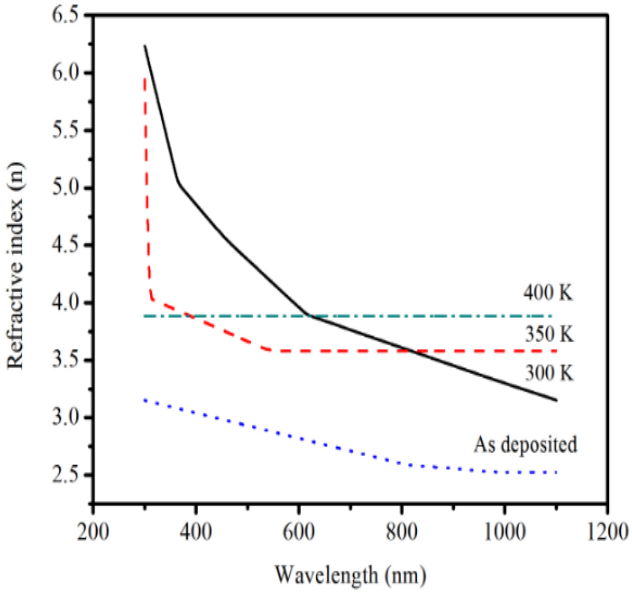

Figure 5: Annealing effects on the refractive index of CIO thin films.

The extinction coefficient (k) with wavelength (λ) of CIO films at different temperatures as shown in Fig. 6. The extinction coefficient of as-deposited film has low values compared to film annealed at 300 K. The extinction coefficient increases with increase in annealing temperature particularly in the NIR region. The factors that contributed in increasing the film transmission with annealing temperature are considered to be responsible for the increase in the extinction co-efficient. Therefore

the extinction coefficient is inversely proportional to transmission [43]

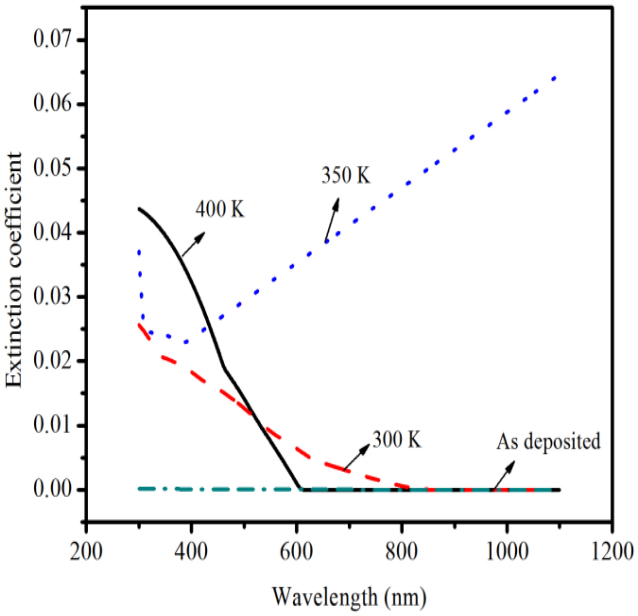

Figure 6: Annealing effects on extinction coefficient of CIO thin films.

4 Conclusion

In this work, nanocrystalline copper doped Indium oxide thin films have been successfully prepared using perfume atomizer technique. The CIO films were annealed for various temperature between 300 to 400 K. The effect of annealing on the structural, electrical, optical, and photoluminescence characteristics of CIO thin film were studied. XRD result revealed that the CIO thin film has a good nanocrystalline cubic structure. High carrier mobility (14.5 cm^2/Vs), a low resistivity ($2.27\times10^{-4}\ \Omega$ cm) and carrier concentration (1.9×10^{20} cm^{-3}) were achieved for the film annealed at 400 K. The optical constants are calculated from the transmission data by PUMA software. All the films exhibit intense PL emission in the UV region. Thus, it is realized that the annealing temperature plays a pivotal role in controlling the structural, electrical and optical properties of CIO films.

Acknowledgement

The authors (V.S and P.P) acknowledge the financial support provided by UGC New Delhi in the form of Rajiv Gandhi National Fellowship (F1-17.1/2011-2012/RGNF-SC-TAM-438/dt.06.06.2012) and MRP (F.No.41-961/2012 (SR) dt.26.07.2012).

Reference

[1] A.Facchetti, T.J.Marks(Eds.), Transparent Electronics From Synthesis to Applications, John Wiley & Sons Ltd.,UnitedKingdom, (2010).

[2] David.S.Ginley,HideoHosono,David.C.Paine(Eds.),Handbook of Transparent Conductors, Springer, NewYork Heidelberg Dordrecht London, (2011).

[3] S.Lany,A.Zakutayev,T.O.Mason,J.F.Wager,K.R.Poppelmeier,J.D.Perkins, J.J.Berry, D.S.Ginley, A.Zunger, Surface origin of high conductivities in undoped In2O3 films, *Physical Review Letters***108**, 016802, (2012).

[4] H. Ohta, M.Orita, M.Hirano, H.Tanji, H.Kawazoe, H.Hosono, Highly electrically conductive indium-tin-oxide thin films epitaxially grown on yttria-stabilized zirconia(100) by pulsed-laser deposition, *Applied Physics Letters***76**, 2740, (2000).

[5] J.J. Loferski, *J. Appl. Phys.***27**, 222, (1956).

[6] F.P. Ko yberg, F.A. Benko, *J. Appl.Phys.***53**, 1173, (1982).

[7] L. Wang, K. Han, M. Tao, *J.Electrochem. Soc.***154**, D91, (2007).

[8] S.C. Ray, *Solar Energy Mater. &Solar Cells***68**, 307, (2001).

[9] D.J. Yoo, S.J. Park, *J. Electrochem. Soc.***143**, L89, (1996).

[10] S. Aygum, D. Cann, Sens. Autuators B **106,** 837, (2005).

[11] S. Anandan, X. Wen, S. Yang, *Mater. Chem. Phys.***93**, 35, (2005).

[12] M.K. Parretta, A. Di Jayaraj, S. Nocera, L. Quercia Loreti, A. Agati, *Phys. Sttatus Sol.***155**, 399, (1996).

[13] W. Zhang, S. Ding, Z. Yang, A. Liu, Y. Qian, S. Tang, S. Yang, *Cryatal Growth***291**, 479, (2006).

[14] J.A. Switzer, H.M. Kothari, P. Poizot, S. Nakanishi, E.W. Bohannan, *Nature*,**425**, 490, (2003).

[15] R.V. Gudavarthy, N. Burla, E.A. Steven, J.Limmer, E. Sinn, J.A. Switzer, *J. Mater. Chem.***21**, 6209, (2011).

[16] K. Ravichandran, P. Philominathan:*Sol.Energy*, **82**, 1062-1066, (2008).

[17] C. Agashe, S. Mahamuni, Semicond. *Sci. Technol.***10**, 172-178, (1995).

[18] D. Beena, R. Vinodkumar, I. Navas, V. Ganasen, A. Yamuna, V.P. Ma-hadevan Pillai, *Journal of Alloys and Compounds***539**, 63-68, (2012).

[19] J.Y. Park, T.H. Kwon, S.W. Koh, Y.V. Kang, Annealing temperature dependence on the physicochemical properties of copper oxide, *Bulletin of the Korean Chemical Socity***32**, 1331-1335, (2011).

[20] L. Changhyun, *Sol. Energy Mater. Sol. Cells***43,**37 (1996).

[21] B. Joseph, *Bull. Mater. Sci.***28**, 487 (2005).

[22] N. Yamada, T. Tatejima, H. Ishizako, T. Nakada, *J. Applied Physics*, **45**, L1179-L1181, (2006).

[23] J.H.W. De Witt, *J. Solid State Chem.***20**, 143, (1977).

[24] G.B. Gon, Z.A. Lez, J.B. Cohen, J.H. Hwang, T.O. Mason, *J. Appl. Phys.***89**, 2550,(2001).

[25] Vipin Kumar Jain, Praveen Kumar, Subodh Srivastava, Y.K. Vijay. Journal of Alloys and Compounds **530**, 132-137,(2012).

[26] A. Nose Kavasoglu, Sertap Karnsoglu and Sensor oktik, *J. Phys Chem. Solids***70**, 521-526,(2009).

[27] M.J. Zhang, L.D. Zhang, G.H. Li, X.Y. Zhang, X.F. Wang, *Appl.Phys. Lett.***79**, 839,(2001).

[28] Y.C. Kong, D. P. Yu, B. Zhang, W. Fang, S.Q. Feng. *Appl.Phys. Lett.***78**, 407,(2001).

[29] D.M Bagnail, Y.F. Chen, Z. Zhu, T. Yao, S. Koyama, N.Y. Shen, T. Goto,*Appl. Phys . Lett.***73**, 1038,(1998).

[30] C.Liang, G. Meng, Y. Lei, F. Phillipp, L. Zhang, *Adv. Mater.***13**, 1330,(2001).

[31] J.J Hop eld, D.G., *Thomas Phys. Rev.***35**,(1961).

[32] D.C. Reynolds, D.C. Look, B. Jobai, C.W. Litton, T.C. Collins, W. Harsch, G. Cantwell, Phys. Rev. B **57**, 12151,(1998).

[33] F.H. Zeng, X. Zhang, J. Wang, L.S. Wang, L.N. Zhang, *Nanotechnology***15**, 596,(2004).

[34] X.P. Shen, H. J. Liu, X. Fan, Y. Yuan, J.M. Hong and Z. Xu, *J. Crys. Growth***276**, 471,(2005).

[35] E.G. Birgin, I. Chambouleyron, J.M. Martinez, *J. Comput. Phys.***151**, 862-880,(1999).

[36] O.S. Heavens, Optical properties of Thin Films, Dover, New York, (1991).

[37] R. Swanepoel, *J. Phys. E: Sci. Instrum*. **16**, 1214-1222,(1983).

[38] D. Poolman, P.F. Smet, *J. Phys. D: Appl. Phys.***36**, 1850-1857,(2003).

[39] Khudiar .AI, Zulfequar .M, Khan .ZH. *Mater Sci Semicond Process*, **15**, 536,(2012).

[40] R. Thielsch, A. Gatto, J. Heber, N. Kaiser, *Thin Solid Films***410**, 86,(2002).

[41] H. Hu, C. Zhu, Y.F. Lu, Y.H. Wu, T. Liew, M.F. Li, B.J. Cho, W.K. Choi, *J. Appl. Phys.***94**, 551,(2003).

[42] T. Tan, Z. Liu, H. Lu, W. Liu, H. Tian, *Opt. Mater.***32**, 432,(2010).

[43] H.A. Mohamed International Journal of Physical Science **7**, 2102-2109,(2012).